PREDICTION OF SAND KINEMATIC PRESSURE AND FLUID-PARTICLE INTERACTION COEFFICIENT AS MEANS OF MONITORING AND ABATING SAND-INDUCED CORROSION IN CRUDE OIL PIPELINES

Samuel Eshorame Sanni*, Sam Sunday Adefila, Ambrose Nwora Anozie

Department of Chemical Engineering, Covenant University, P.M.B. 1023, Ota, Ogun State, Nigeria

Corresponding author's email: adexz3000@yahoo.com

Mobile no: +234 8034332497

ABSTRACT

Sand-induced corrosion and scaling of petroleum pipes is a serious situation that barely knows any solution by conventional or new methods of corrosion control. This is because, the mechanism behind sand corrosion and scaling of petroleum pipes is yet to be unravelled. Rather than avoid the situation, the integration of sand filters in petroleum lines also contribute to the problem. In this work, a three phase model was used to simulate upstream flow conditions where sand is produced alongside water and crude oil. The best flow conditions for the system were established and the model was used to make parametric predictions of the kinematic pressures, interaction coefficients and interaction forces in order to find out the effect of kinematic pressure of the sand phase in relation to conditions that favour sand deposition, corrosion and scaling of petroleum pipes. The model results show that, on a 3-hour basis, periodic checks need be conducted with special attention given to the 12-18 m points where sand kinematic pressures and interaction coefficients of the components require flow adjustments in order to avoid situations leading to unfavourable flow or pipeline wear.

Key words: Interaction Coefficients; Kinematic Pressure, Sand-crude oil-water system; Sand Deposition; Sand-induced Corrosion; Three phase Model

1. INTRODUCTION

Several works on multiphase flows include particles of different orientations where the solid particles are not sand. However, the knowledge gained from the research works have helped to understudy and understand the broad subject of sand transport during upstream petroleum production operations. Multiphase flow models such as those of Doan et al. [1, 2] were developed to tackle situations of laminar flows where sand particles are carried along with the flowing oil however, these models have their shortcoming as a result of the number of components considered, datum level, lack of incorporation of the effect of eddies in the model development, pipe orientation in space and the effect of turbulence. Conventional ways of separating sand from crude oil and water involves the use of sand pacs or filters which get clogged with particles over time with resultant closure in pipe area, sand accumulation, formation of sand scales owing to sand build-up/deposition which subsequently results in sand-induced corrosion. Investigations on multiphase flow transport of particles and fluids have not been studied in relation to the influence of pressure drop on sand deposition (sand-induced corrosion) and kinematic pressure of sand in sand-crude oil and water systems. This knowledge is necessary as it informs the operator of what decisions to make in line with regulating the kinematic forces and pressures when faced with situations leading to sand-induced corrosion/scaling. In well lines, deposited sand particles have the tendency of sticking to well lines when the mixture becomes stratified hence the need to seek proper understanding of the parametric variations that bring about such instabilities, two of such are the kinematic pressures and forces that can be influenced by pressure drop which also gives rise to sand corrosion problems. Till date, corrosion engineers are yet to unravel the conditions that lead to flow stratification during sand-crude oil and water transport [3]. At such condition, water being a corrosion stimulant/electrolyte rests on the pipe wall and dissolves sand particles which may lead to the formation of silicic acids that in turn cause electrochemical corrosion. Also, mechanical corrosion may occur for crystalline insoluble

sand particles which may grind off metallic grains off the pipe, thus leading to mechanical wear. According to Ko et al. [4], concentrations of particles and carrier velocity of the fluid are important parameters to pay attention to during fluid-particle flows; this in turn suggests that fluid-particle pressures and forces cannot be undermined thus, solid particles in a turbulent stream tend to drop out of suspension and form a solid bed when the flow velocity is below the particle-lift forces required to keep the particles in suspension. When this happens a bed of solids may begin to build-up on the pipe wall which may result in sand scales when such condition subsists; this bed of solid particles may begin to slide or move again when the flow velocity exceeds the critical deposition velocity of the particles [5]. Also, based on the work of Stuhmiller [6], interfacial force effect becomes significant when the entire mix becomes stratified. Smart [7] estimated the flow velocities of particles that make-up black powder in petroleum fluids (water, diesel, crude oil and natural gas). The particles include $FeCO_3$, FeO, FeS, Fe_3O_4, sand, weld spatter and salt which agglomerate into a solid mass agglomerate to form black powder in petroleum fluids (water, diesel, crude oil and natural gas). The work shows that while the estimated velocities are used as a means of launching pigs for corrosion control, the velocities obtained only showed slight differences which is as a result of their close densities. Vortex simulations of a two-phase dilute particle laden layer was used to establish a correlation between fluid-particle motion and transmission of turbulent kinetic energy in both phases Horrenda and Hardalupas [8]. Results from the simulation gave reductions in fluid turbulence as a result of the particle Stokes number which was influenced by particle concentration distribution and the relative velocity between both phases. Wang [9] studied the effect of turbulence caused by a two-phase point-force; in this work, particle trajectories were defined by the Langrange method. Findings from the work, confirm that streaky cloudy orientations of settling particles may be weakened by increased inertia forces. The study of Capecelatro and Desjardins [10] involves numerical computations

of the complex multiphase flow dynamics occurring in a slurry pipeline; their investigations were centered on determining conditions that lead to particle suspension and deposition. Their results also confirmed that, for slurry flows where the flow velocity is below the critical particle deposition velocity, three distinct layers may become evident and these include a rigid bed load layer, a particle-particle shear flow layer and a freely-suspended particle layer. The estimation of particles velocity in a slurry pipeline was investigated by Hashemi et al. [11]. Solid concentrations were measured alongside their velocities. The results show that concentration variation of solids in the pipe were localized near the pipe wall and increased with the carrier mix velocity. Messa et al. [12] also carried out a numerical simulation of conditions necessary for safely transporting suspended solid particles in a slurry pipeline. The work of Parsi et al. [13] is a review of model applications to sand particle erosion of oil and gas pipelines in which two major concerns (pipe blockage and pressure drop) were identified as problems associated with pipe erosion. They also added that, sand corrosion is a mechanical wearing process by which some of the metal of the pipe is lost owing to repeated impact of sand particles hardness on the pipe walls and this may eventually result in pipeline failure and environmental problems. An experimental study was conducted to investigate conditions that lead to sand deposition in a horizontal slurry pipeline where sand was transported in a suspension. From their study, they estimated the sand threshold and minimum deposition velocities [14]. Yang et al. [15] carried out numerical simulations of the transport and progressive reactions occurring in a microreactor. Segmented slug flow patterns were simulated using OpenFOAM in order to determine the circulation patterns and fluid wetting characteristics of an existing slug in a microreactor. Particle concentrations, pressures and estimated velocities from their simulations showed that, the concentration patterns obtained were influenced by Peclet number, while particle transport was largely influenced by the Damkholer number which are measures the inherent heat and mass transfer forces in

the system respectively. A mechanistic model that is capable of predicting particle optimum/threshold velocity, critical velocity and sand holdup in pipelines and wells was developed [16]. The study was aimed at solving sand management problems caused by sand particle deposition, bed formation, erosion, pressure loss and poor well productivity which eventually translate to increased loss due to maintenance and repairs. The study carried out by Choong et al. [17] is a comparative analyses of four models for multiphase flows. The spreadsheet-based model has the ability to predict sand critical settling velocity and the onset of sand deposition. A vibration technology for detecting sand particles which uses time-frequency analysis and sand digital band filter was established by Wang et al. [18]. Sand-water and oil-water-sand movements were tracked using the vibration signals from a sensor. They were able to establish a good correlation between the amplitude/peaks of the vibrations and sand concentration in the multiphase system. Science Media Centre [19] discussed the types the causes of internal and external corrosion, cathodic disbondment as well as the use of intelligent pigs and high resolution Supervisory Computer Aided Data Acquisition (SCADA) systems in corrosion detection/monitoring. Samini and Zarinbadi [20], is a study that bothers on pipe corrosion caused by CO_2, H_2S, Cl, and O_2. Their findings suggest the use of intelligent pigs as a possible way of controlling internal corrosion. James and Bushman [21], discussed pipe corrosion and control by via the use of impressed current or sacrificial anode methods. Despite these strides (i.e. the existence of model and conventional sand control methods), sand detection and prediction tools still cannot give sand mass, sand volume and the rate of sanding for oil field related problems and these parameters help to pass a clear judgment on the corrosion and scaling tendencies of sand during multiphase flow operations, especially in situations where pressure drop becomes significant [22].

2. DATA MEASUREMENT

Data was obtained from the field using flow facilities set up by ADDAX Petroleum, Owerri, Imo state, Nigeria. Using a pump positioned at the well bore, hydrocarbon was transported from a reservoir into a 24 m well line which links the wellbore to the tubing head. The line comprises of sand screens/filters positioned at the pipe inlet, 8 and 14 m points of the pipe that helped to filter coarse, medium and fine sand particles respectively. A SCADA machine was used to generate data from the well. Feeder lines were then used to transport the reservoir fluid to a separator from which the quantity of crude oil, water and sand were determined. The average particle hardness of sand (i.e. 800 Vickers) was measured using a pyknometer. The data in Table 1 gives flow measurements from the well. The injection and flowing tubing pressures were 1100 and 793 psia.

3. THE THREE PHASE MODEL

A three-phase model was developed whose origin lies in the Doan et al. [1, 2] and Sanni et al. [23] models was developed and used to carry out numerical estimations of the flow scenario.

$$\frac{\partial}{\partial t}(\phi) + \frac{\partial}{\partial z}(\phi w_s) = 0 \tag{1}$$

$$\frac{\partial}{\partial t}(\sigma) + \frac{\partial}{\partial z}(\sigma w_s) = 0 \tag{2}$$

$$\frac{\partial}{\partial t}(\varepsilon) + \frac{\partial}{\partial z}(\varepsilon w_f) = 0 \tag{3}$$

$$\frac{\partial}{\partial t}(\theta) + \frac{\partial}{\partial z}(\theta w_w) = 0 \tag{4}$$

$$\frac{\partial}{\partial t}(\phi' w_s) + \frac{\partial}{\partial z}(\phi' w_s w_s) = -(\phi' g) - \frac{\phi'}{\rho_s}\frac{\partial P_s}{\partial z} + \frac{\beta}{\rho_s}(w_f - w_s) - \frac{P_k}{\rho_s}\frac{\partial \phi'}{\partial z} \tag{5}$$

$$\frac{\partial}{\partial t}(\varepsilon w_f) + \frac{\partial}{\partial z}(\varepsilon w_f w_f) = -(\varepsilon g) - \frac{\varepsilon}{\rho_f}\frac{\partial P_f}{\partial z} + \frac{\beta}{\rho_f}(w_f - w_s) \quad (6)$$

$$\frac{\partial}{\partial t}(\theta w_w) + \frac{\partial}{\partial z}(\theta w_w w_w) = -(\theta g) - \frac{\theta}{\rho_w}\frac{\partial P_f}{\partial z} + \frac{\beta}{\rho_w}(w_f - w_w) \quad (7)$$

The parameter ϕ' is a total particle term i.e. $\phi' = \phi + \sigma$ (8)

Total fluid concentration £ = θ + ε (9)

$\sigma, \theta, \phi', w_w, \rho_w, P_w$ are the sand deposit concentration, percent water, total sand concentration, water velocity, water density and water pressure respectively.

3.1. Boundary Conditions and Model Calibration

Boundary conditions for the crude oil, sand and water system, were established for the model. The model was also calibrated using the approach discussed in Sanni et al. [23, 24]. The oil boundary conditions for the inlet and outlet sections of the pipe were calculated using (10) and (11). The inlet and outlet boundary conditions for water were determined using (12) and (13), while (14) and (15) were used to determine the inlet and outlet sand concentrations respectively.

$$\varepsilon_{inlet} = \frac{vol.oil}{vol.oil + vol..sand + vol.water)} \quad (10)$$

$$\varepsilon_{outlet} = (\frac{vol.oil}{vol.sand + vol.oil + vol.water}) \quad (11)$$

$$\theta_{inlet} = \frac{vol.water}{vol.oil + vol.sand + vol.water)} \quad (12)$$

$$\theta_{outlet} = (\frac{vol.water}{vol.sand + vol.oil + vol.water}) \quad (13)$$

$$\phi'_{inlet} = (\frac{vol.sand}{vol.sand + vol.oil + vol.water}) \quad (14)$$

$$\phi'_{outlet} = \left(\frac{vol.sand}{vol.sand + vol.oil + vol.water}\right)` \quad (15)$$

Correlations for eddy molecular and eddy diffusivities were then used to determine the molecular and momentum diffusivities in the laminar sub-layer, the transition zone and the turbulent core region.

3.2 Correlation for Estimating Concentration and Velocity of Components

Equation 16 was used to estimate the concentration and velocity distribution of the components along the pipe. Here, equal change in concentrations were assumed based on the estimated inlet and outlet concentrations for each of the components along an equal length interval of 6 m.

$$j_{k+1}^{,l+1} = j_{k-1}^{,l+1} - (j_{k-1}^{,l-1} + j_k^{\,l})\frac{1}{4} \quad (16)$$

Where j_{k+1} is the concentration to be determined at a position, j_{k-1} and j_k are the inlet and outlet concentrations of the components. The calculated concentration values are: 0.111, 0.110875, 0.11075, 0.110625, 0.1105 for sand, the estimated oil concentrations are 0.52804347, 0.52802435, 0.52800523, 0.52798611, 0.5279670 while for water, the corresponding concentrations are 0.361, 0.360625, 0.36025, 0.359875, 0.3595 at 6 m interval and t = 1 h respectively.

3.3. Finite Difference Solution to the mass conservation equations

The model equations were solved using finite difference equations generated for the sand. Water and oil; see (17-20) respectively.

$$\phi_{k+1}^{,l+1} = \psi(\phi_k^{,l+1} - 2\phi_k^{,l} + \phi'^{\,l}_{k-1}) + \phi_k^{,l} \quad (17)$$

$$\theta_{k+1}^{\,,l+1} = \psi(\theta_k^{\,,l+1} - 2\theta_k^{\,,l} + \theta'_{k-1}{}^{l}) + \theta_k^{\,,l} \quad (18)$$

$$\varepsilon_{k+1}^{\,,l+1} = \psi(\varepsilon_k^{\,,l+1} - 2\varepsilon_k^{\,,l} + \varepsilon'_{k-1}{}^{l}) + \varepsilon_k^{\,,l} \quad (19)$$

$$\psi = \frac{D_T \Delta t}{2\Delta z^2} \quad (20)$$

Where $_k$, $_{k+1}$ and $_{k-1}$ represent time steps and $_l$, $_{l+1}$ and $_{1-1}$ indicate positions along the pipe axis. D_T is the sum of molecular and total diffusivities. Considering the 6, 12 and 18 m sections of the pipe at t = 1 h implies, the calculated sand concentration from the field (0.1105) was compared with that obtained from the model (i.e. 0.11075) which shows that the model's accuracy is above 99.77 %. The calculated ψ = 5.66 x 10^{-4}. An average value for sand diffusivity, that is, 1.132 x 10^{-5} m^2/s was calculated from the estimated sand diffusivities at the pipe inlet and outlet, so as to simplify the simulation. For water, the average total diffusivity between the inlet and outlet is 3.86 x 10^{-5} and from (20), ψ = 1.93 x 10^{-3}. Then at the field, the % volume of water at the pipe exit = 0.3595 while the predicted volume % of water = 0.359875. Applying (19) to the conservation equation for the oil, the average sum of eddy and molecular diffusivities is given as 5.8495 x 10^{-5} while ψ = 2.925 x 10^{-3} for oil.

3.4. Finite Difference Solution to the Momentum Equations

The sand oil and water velocities were estimated by obtaining the products: $\phi' w_s$, εw_f and θw_w giving 0.078, 0.371 and 0.253 m/s as the inlet velocities for sand oil and water respectively, while their corresponding outlet velocities are 6.67 x 10-5, 3.2 x 10-4 and 2.2 x 10-4 m/s. These values were used as boundary conditions for the finite difference equations (21-23).

$$h_{i+1}^{\,,l+1} = \psi(h_i^{\,,l+1} - 2h_i^{\,,l} + h'_{i-1}{}^{l}) - \frac{1}{2}\{(\phi' g) - \frac{\phi'}{\rho_s}\frac{\partial P_s}{\partial z} - \frac{\beta}{\rho_s}(w_f - w_s) - \frac{P_k}{\rho_s}\frac{\partial \phi'}{\partial z}\} + h_i^{\,,l} \quad (21)$$

$$\eta_{i+1}^{l+1} = \psi(\eta_i^{l+1} - 2\eta_i^{l} + \eta_{i-1}^{l}) - \frac{1}{2}\{(\varepsilon g) - \frac{\varepsilon}{\rho_f}\frac{\partial P_f}{\partial z} - \frac{\beta}{\rho_f}(w_f - w_s)\} + \eta_i^{l} \quad (22)$$

$$\Phi_{i+1}^{l+1} = \psi(\Phi_i^{l+1} - 2\Phi_i^{l} + \Phi_{i-1}^{l}) - \frac{1}{2}\{(\varepsilon g) - \frac{\varepsilon}{\rho_f}\frac{\partial P_f}{\partial z} - \frac{\beta}{\rho_f}(w_f - w_s)\} + \Phi_i^{l} \quad (23)$$

Where $h = \phi' w_s$, $\eta = \varepsilon w_f$ and $\Phi = \theta w_w$. Equations 21-23 are the momentum equations for sand, oil and water respectively.

RESULTS AND DISCUSSION

In Figure 1, it could be seen that the optimum operating condition for the transport of the reservoir fluid from the well bore to the flowing tubing head lies between 793 psia and 1100 psia. This is because, within these inlet and exit pressure limits, the least quantity of sand (1.22 lb/mbbl) and the highest quantity of oil were produced unlike what was produced at other pressure limits, hence reason the flow situation at these pressure limits were used to carry out the simulation.

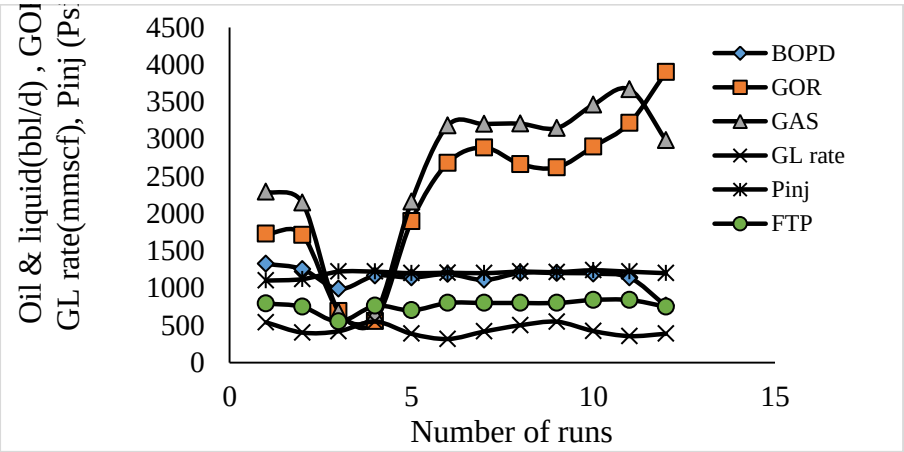

Figure 1: Injection Pressure, Produced Oil, Liquid, Gas, GOR & Gas-liquid Rate per Day for the Different Experimental Runs

Concentration variation

The concentrations of the components are measures of their densities. The concentration of oil is highest while that of water is next with that of sand being least. In a plug flow system, there are no changes in concentration with time since at different times, the components concentrations are the same at specific points, whereas changes are evident with respect to position (Figure 1). From the inlet to the exit, sand concentration dropped by 0.0005 which is about 0.05%. For oil, the concentration change from the inlet to the exit of the pipe is about 0.0003 i.e. 0.02%. Considering the values close to the exit i.e. the 18 m point, the reduction in the carrier fluid pressure is most significant, which may be due to opposition to flow or the possibility of a constriction in the pipe or sand buildup between both points. For water, the concentration seems to be lower than that of oil but higher than that of sand owing to their densities. The concentration for water varied between 0.361 - 0.3595 for water from the inlet to the exit giving a change of 0.0015%; the results are corroborated by Doan et al [2].

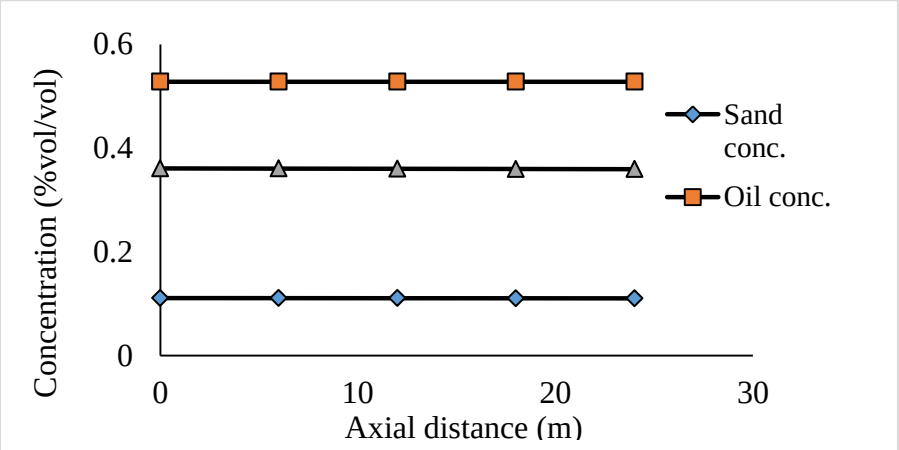

Figure 2: Oil, Sand and Water Volume Fractions along the Pipe Axis

Velocity distribution

In Figure 2, the estimated sand velocities change with position although these values were found to be constant at different times simply because, particles were assumed to be of same shape and density. Between successive points, the values recorded are 0.078 m/s, 0.0585 m/s,

0.390 m/s, 0.019 m/s and 0.000067 m/s, at the 0, 6, 12, 18 and 24 m sections of the pipe respectively. The changes are more evident from the 12 m point to the exit i.e. 49.9 % between the 12 and 18 m points while it is 99.6% between the 18 and 24 m points. Oil velocities varied between 0.370 and 0.00032 m/s from the pipe inlet to its exit respectively, giving a change of 0.3697 m/s while for water, the velocities at the inlet and pipe outlet are 0.253 m/s and 0.00022 m/s. From 0 and 6 m, the change in water velocity is 0.063 m/s (i.e. 24.9%). It changed by 33.2% between 6 and 12 m and was about 49.9% at the 12-18 m points; aft the 18-24 m section, the recorded change in water velocity is 99.1%. These changes resulted from the drop in the flow rate of the career oil which subsequently affected the flow rate of the water at different points of the pipe.

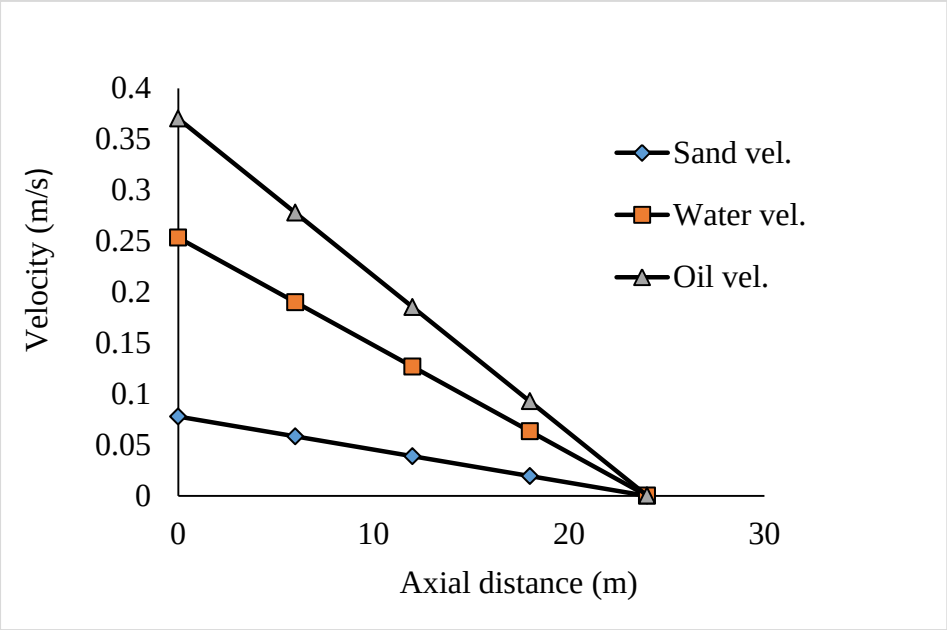

Figure 3: Sand, Oil and Water Velocities along the Axial Distance

Sand phase pressure

The estimated pressures of the sand particles along the pipe show that, the pressure drop is significant at the 18-24 m points as seen in Figure 4. This results from the significant change

in sand velocity along the pipe owing to the lower carrier fluid pressure forces. At the 18 m point, particles deposition is high owing to the resistance offered by the viscous forces of the fluid thus causing particles to settle towards the pipe wall. Between the 18-24 m point, sand deposition and water transport towards the pipe wall may result in sand accumulation and dissolution in H_2O; also, mechanical wearing of the pipe may occur when a moving bed is dragged along the pipe at such critical condition. The pressure exerted on the sand was high up to the second hour after which it dropped throughout with slight variations from the third to the sixth hour.

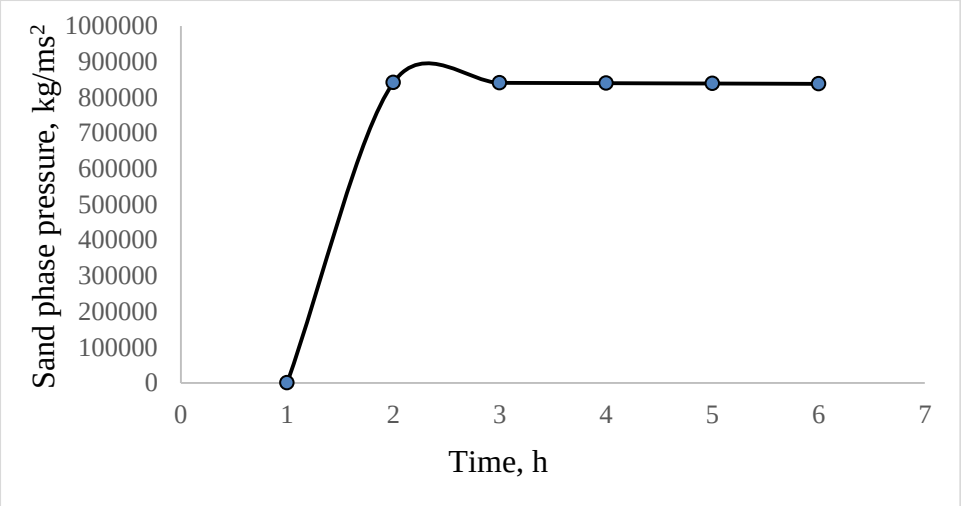

Figure 4: Change in Sand phase pressure along the axial distance

Figure 5, gives an illustration of the change in oil phase pressure along the axial distance which confirms what is seen in Figure 4. Figure 5 simply complements what is seen in Figure 4 by exposing the positions along the pipe where production engineers need to apply caution. When the change in pressure of the carrier oil is high, it subsequently affects that of the entrained sand and water thus causing the particles and water to drift towards the pipe wall.

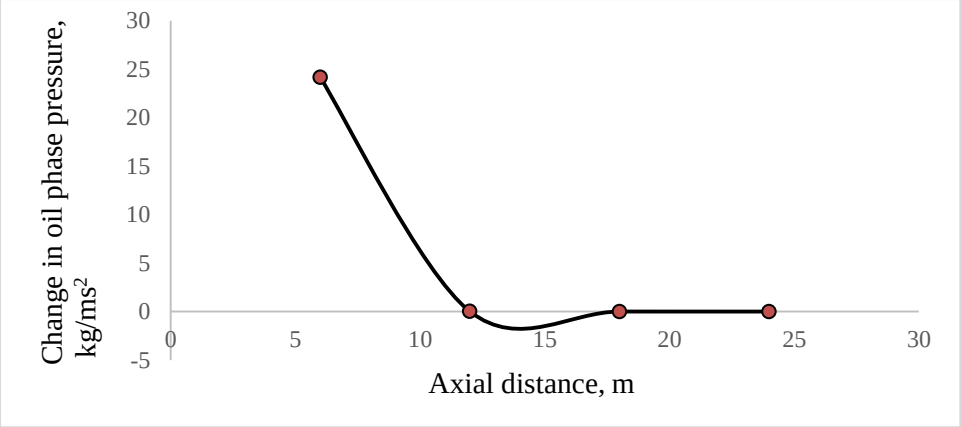

Figure 5: Change in Oil phase pressure along the axial distance

The water Phase Pressure seems to show only slight reductions owing to the various interactions occurring in the stream (Table 1). Oil and water do not mix hence, a repulsive force exists between the two fluids; this creates a void/vortex which is likely filled by sand. One would expect that sand remains the lowest layer under critical flow conditions however, this is not so because, water will tend to drift farther away from oil owing to the measure of repulsion that exists between them i.e. the higher it is, the farther away water goes from the oil with some sand rolling over to replace the repelled water due to a higher momentum imparted on the sand which gives it a higher velocity relative to water at some points in the mixture.

Table 1: Water phase pressure along the axial distance for 6 h

	Water phase pressure (kg/ms^2)				
t (h)	**0 m**	**6m**	**12 m**	**18 m**	**24 m**
1	2737153.623	2734310	2731467.016	2728623.7	2725780
2	2737153.623	2734310	2731467.016	2728623.7	2725780
3	2737153.623	2734310	2731467.016	2728623.7	2725780
4	2737153.623	2734310	2731467.016	2728623.7	2725780
5	2737153.623	2734310	2731467.016	2728623.7	2725780
6	2737153.623	2734310	2731467.016	2728623.7	2725780

Sand kinematic pressure

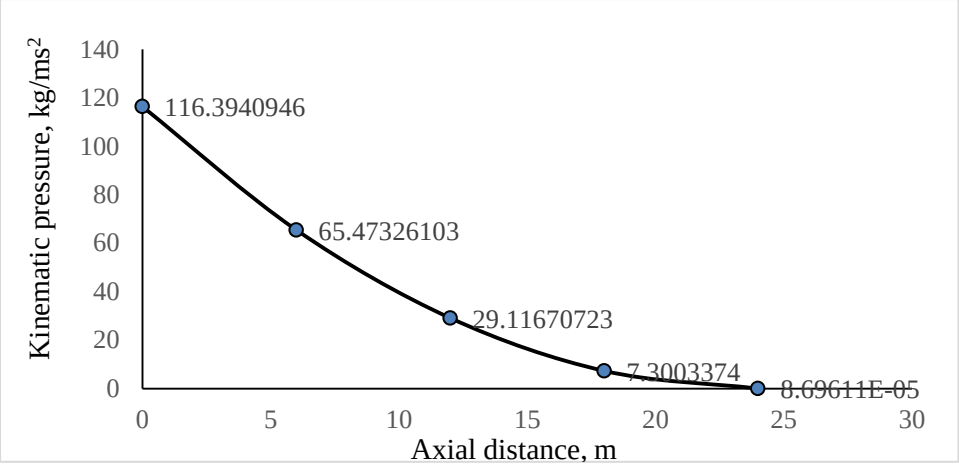

Figure 6: Kinematic Pressure for Sand along the Axial Distance

Figure 6 is a graphical illustration of the kinematic pressure of sand along the pipe axis. The kinematic pressure of sand varied from 116.39 - 8.69 kg/ms^2. The changes showed that the sand kinematic pressure at the 6 m point is 1.8 times less than the previous value, at the 12 m point, it is about 2.3 times the previous value. The kinematic pressure dropped by 4 times the previous value at the 18 m point. Between the 18 m point and the exit, the ratio of the kinematic pressure values estimated is 84004.6. Therefore, serious caution is to be applied (i.e. the need to integrate a booster/pump at between the 12-18 m point) to make up for the lost kinetic energy of the flowing mix in order to boost the sand kinematic pressure

Table 2: Kinematic pressure force per unit mass along the pipe axis for 6 h

	Kinematic pressure force (ms^{-2})				
t (h)	**0 m**	**6m**	**12 m**	**18 m**	**24 m**
1		4E-07	1.8E-07	4.5E-08	5.3E-13
2		4E-07	1.8E-07	4.5E-08	5.3E-13
3		4E-07	1.8E-07	4.5E-08	5.3E-13
4		4E-07	1.8E-07	4.5E-08	5.3E-13
5		4E-07	1.8E-07	4.5E-08	5.3E-13
6		4E-07	1.8E-07	4.5E-08	5.3E-13

In Table 2, changes in kinematic pressure per unit mass vary between 4 x 10^{-7} to 5.3 x 10^{-13} ms^{-2} from the inlet down to the exit. This difference is very high and is very significant

between the 18-24 m section of the pipe and this agrees with the results in Figure 6; the value at the 0 m point cannot be obtained because the pressure gradient is undefined.

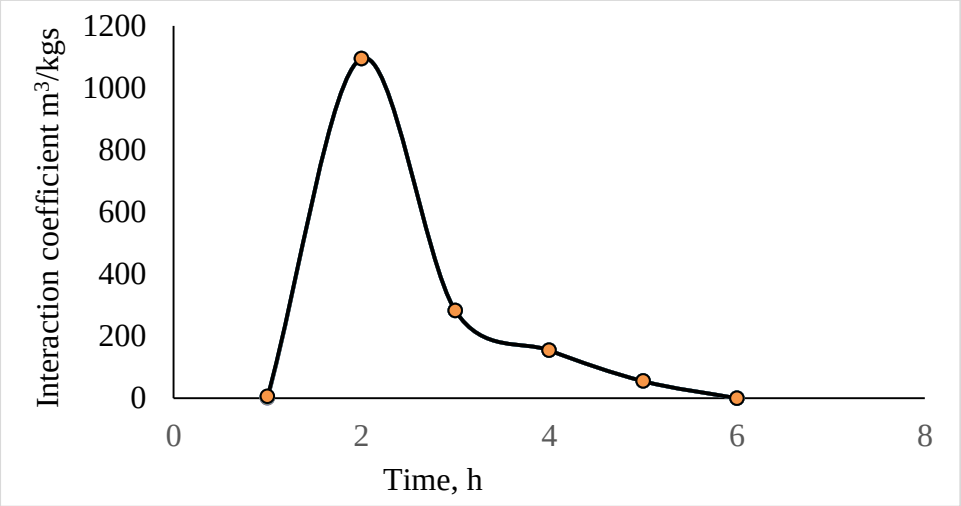

Figure 7: Interaction Coefficient Variation along the Axial Distance

Based on the results shown in Figure 3, the estimated interaction coefficients also confirm the results obtained in Figure 3 where sand phase pressures began to drop significantly after 2 hours. This helps to also lay emphasis on the need to take precautionary measures after at 3 hours of production time as the estimated coefficients show that, at low pressures where flow stratification becomes significant, the relative velocity or slip between any two pair of components or parallel phases becomes very small thus resulting in low interactions among the carrier oil, sand and water, hence, it is necessary to conduct periodic monitoring or checks on the flow at 3-hour interval since the level of interactions dropped further at 6 hours.

Table 3: Interaction forces per unit mass along the axial distance

z (m)	oil-sand (ms^{-2})	sand-oil (ms^{-2})	water-sand (ms^{-2})	sand-water (ms^{-2})	water-oil (ms^{-2})	oil-water (ms^{-2})
0	0.18221	0.09381	0.09602469	0.0563063	0.0639518	0.07283804
6	0.03523	0.01814	0.01856735	0.0108874	0.0123657	0.0140839
12	0.01286	0.00662	0.00677749	0.0039741	0.0045137	0.00514088
18	0.0023	0.00118	0.00121254	0.000711	0.0008075	0.00091971
24	2.1E-09	1.1E-09	1.1317E-09	6.636E-10	7.397E-10	8.4248E-10

Table 3 gives the interaction forces for any pair of components in the mix. The interaction forces are measures of the relative densities of the components. It is highest for oil-sand because between this pair exists the highest slip. The interaction forces as estimated in Table 3 in order of decreasing slip between pair of components are: oil-sand, water-sand, sand-oil, oil-water, water-oil and sand-water. What this implies is that, there is every tendency to have water associated with sand during critical conditions i.e. below the critical deposition velocity and this subsequently imparts on pipe integrity when the flowing stream is stratified. Corrosion may exist in the form of fretting corrosion due to sand deposition. Furthermore, if the condition leading to flow stratification is not controlled, stress corrosion cracks may be induced when a bed load of sand is formed; this also reduces the service life of the pipe which may lead to early replacement or huge costs incurred from work-over operations.

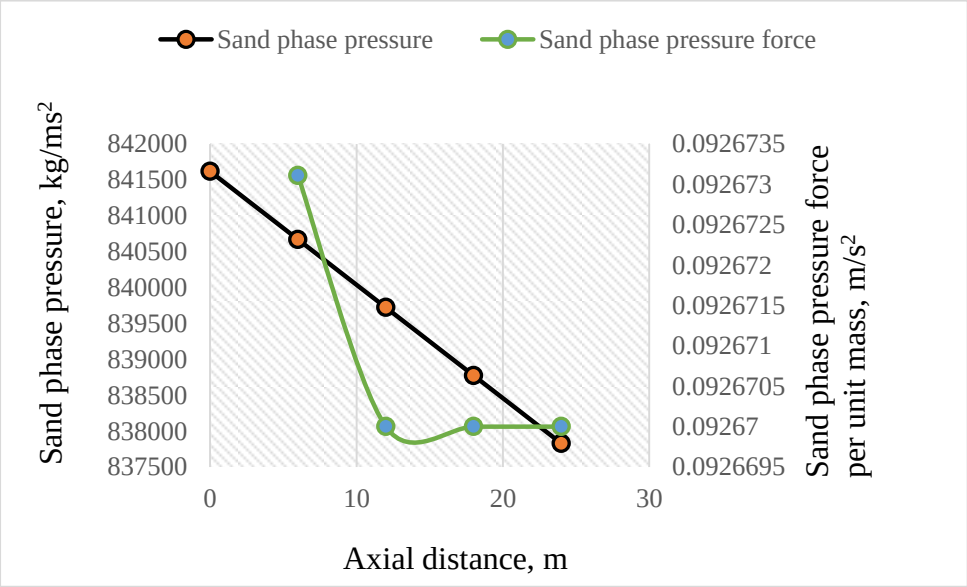

Figure 8: Sand phase pressure and sand phase pressure force along the axial distance

In order to bridge the gap or further understand the relationship between the sand phase pressure and the sand phase pressure force per unit mass, the plot in Figure 8 was made. Both parameters reduced in value from the 0 m point to the exit. However, the points of intersection are sand phase pressure equals the sand phase pressure force per unit mass. The

top equilibrium point is the critical point below which the sand particles begin to withdraw from the turbulent core region into the transition zone; above this point is the turbulent core region. The region bounded by the line and curve is the transition zone; it is also enclosed by the two points of intersection. Below the lower point of intersection is the laminar layer.

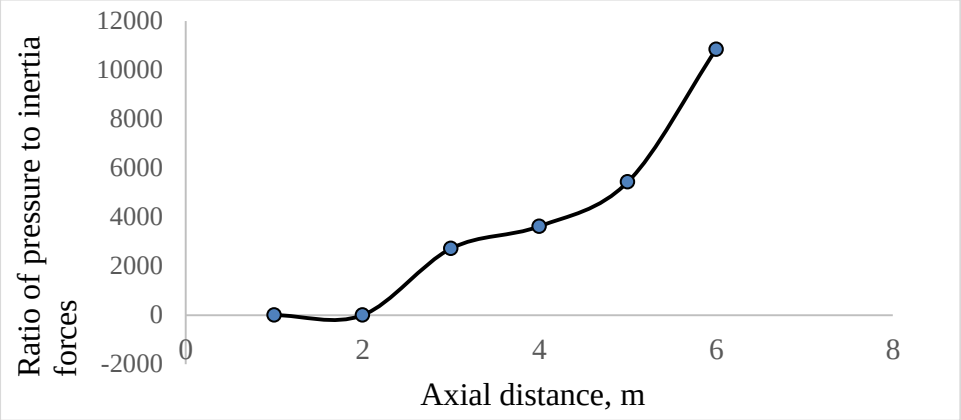

Figure 9: Ratio of pressure to inertia forces for 6 h

Figure 9 shows the pressure force competition against the inertia forces of the carrier oil for 6 hours. Again, within the first two hours, the pressure forces were very low relative to the inertia forces, however, higher pressure forces began to result relative to inertia forces and when this results, the tendency for sand deposition is increased.

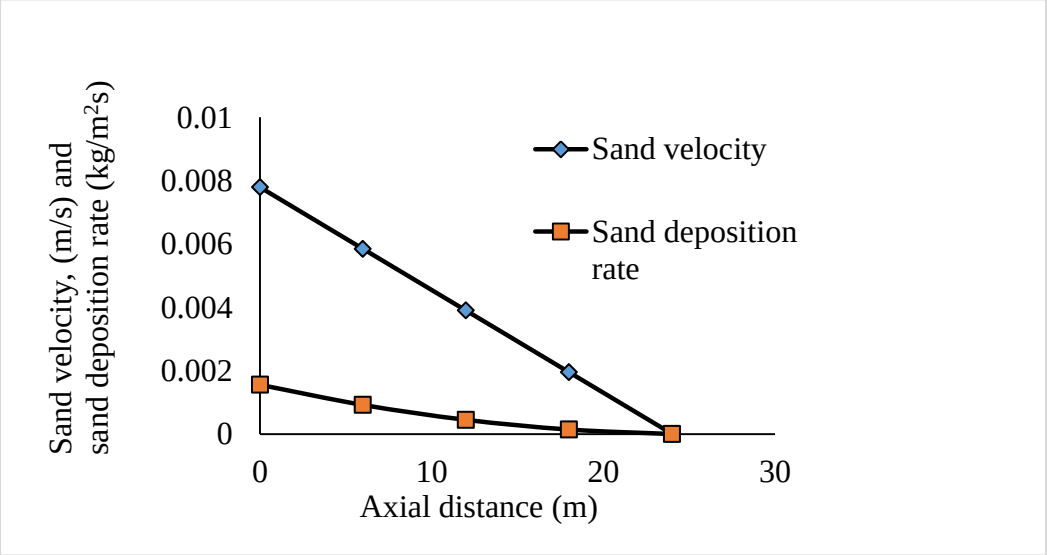

Figure 10: Sand Deposition Rate and Sand Velocity for 90% Drop in Oil Velocity

The plot in Figure 10 was then obtained by tuning the model to a situation where the stream becomes laminar. This was done by assuming determining the Reynolds number of the oil influx. 90 % drop in oil velocity was assumed in order to mimic the flow scenario described by Doan et al. [2] where a Reynolds number of 1000 was ideal to describe turbulence in a petroleum fluid carrying sand. Within this condition, the sand deposition rate was estimated alongside sand velocity along the axial distance. The results are in good agreement with what was reported by Sayeed et al. [25] for velocity distribution and wax deposition rate in a petroleum pipeline. As sand velocity dropped, the rate of sand deposition reduced, this is not because sand particles were not dropping but this only occurred at a slower rate, although, sand deposition is usually high only at the onset of deposition but becomes lower as more and more particles settle towards the pipe wall. The continuous drop in sand deposition rate may be due to hindered settling of particles in close contact such that the collisions between close particles in contact may result in resuspension. Furthermore, the low deposition rate recorded for sand may be as a result of the bed of particles that would have been formed under such condition. **CONCLUSION**

The three phase model helped to establish a good relationship among the interaction forces, interaction coefficient and sand pressure forces. Furthermore, the relationship that exists among these variables can be exploited as a means of abating sand corrosion and scaling tendencies in pipelines transporting crude oil, sand and water from an oil well. For the well, when the operating pressures between the pipe inlet and outlet is in the range of 1100 -793 psia, periodic checks should be made on a 3-hour basis in order to guide against unforeseen consequences which may give rise to emergency short downs if such conditions are allowed to linger beyond permissible limits. Also, the 12-18 m points are points for improving on the lost pressure of the system; this can be done by integrating a pump on the line which will help

to boost the inertia forces at those points of the pipe. Furthermore, higher sand kinematic pressures are desired to abate sand corrosion tendencies and allow for safe and reliable transport of sand and water because, literature has it, that, sand (SiO_2), besides having the ability to cause mechanical wearing of pipes, has a measure of solubility in water, which is a stimulant for electrochemical corrosion.

ACKNOWLEDGEMENT

The authors appreciate the Department of Petroleum Resources, Nigeria for providing the platform to liaise with ADDAX Petroleum Ltd. which made it easier for me to have direct access to data generated on the field with standard equipment procedures. Also, we appreciate the role of Covenant University in terms of her financial support and sponsorship throughout this research.

NOMENCLATURE

Symbols	**Designation**	**Unit**
Letters		
A	Cross-sectional area	m^2
g	Gravitational acceleration	ms^{-2}
P_f	Oil phase pressure	$kgm^{-1}s^{-2}$
P_k	Kinematic pressure	$kgm^{-1}s^{-2}$
P_s	Sand phase pressure	$kgm^{-1}s^{-2}$
P_w	Water phase pressure	$kgm^{-1}s^{-2}$
q_f	Volume flow rate of oil	m^3s^{-1}
q_s	Volume flow rate of sand	m^3s^{-1}
q_w	Volume flow rate of water	m^3s^{-1}

t	Time	hrs or s
V_m	Volume of mixture	m^3
w_o	Oil velocity	ms^{-1}
w_s	Sand velocity	ms^{-1}
w_w	Water velocity	ms^{-1}
z	Axial distance	m
β	Fluid-particle interaction coefficient	kgm^3s^{-1}
Δz	Change in length	m
ε	Oil concentration (volume fraction)	-
ϕ	Suspended sand concentration (volume fraction)	-
σ	Deposited sand concentration (volume fraction)	-
ϕ'	Total sand concentration (volume fraction)	-
θ	Water concentration (volume fraction)	-
ρ_f	Oil density	kg/m^3
ρ_s	Sand density	kg/m^3
ρ_w	Water density	kg/m^3

List of Abbreviations

BLPD	Barrels of liquid per day	bbl/day

BOPD	Barrels of oil per day	bbl/day
BSW	Base sediment & water	%
Choke	Choke size	-
FTP	Flowing tubing pressure	psia
Gas	Amount of gas produced	scf/d
GOR	Gas oil ratio	-
GL rate	Gas-liquid rate	scf/day
Pinj	Injection pressure	psia
PTB	Parts per thousand barrel	pptb

REFERENCES

[1] 'Simulation of sand transport in a horizontal well', International conference on horizontal well technology' Q. Doan, A. Farouq, A. George and M. Oguztoreli, Calgary, Canada, November pp. 18-20, 1996.

[2] 'Sand deposition inside a horizontal well - a simulation approach', Q. Doan, A. Farouq, A. George and M. Oguztoreli, M, *SPE Journal*, **39,** 33-40, 2000.

[3] 'Oil-water separation phenomenon due to corrosion cavity and scale and scale sediment build-up in horizontal pipelines', N. Abdullahi, Ph.D Thesis, 2012, Cranfield University, UK.

[4] 'Lift-off of a single particle in an oldroyd-b fluid' T. Ko, N. Patankar and D. Joseph, University of Minnesota Computer Institute, 2001, Minneapolis, USA.

[5] 'Sand transport modeling in multiphase pipelines', T.J. Danielson, Proceeding of Offshore Technology Conference, April 30-May 3, 2007, Houston, Texas, USA. Http//dx.doi.org/10.4043/18691-MS.

[6] 'The influence of interfacial pressure forces on the character of two phase flow model equations' J.H. Stuhmiller, *International Journal of Multiphase Flows*, **3,** 551-560, 1977.

[7] 'Calculating velocity for solid particle movement in oil and gas pipelines', J. Smart, ***(In):*** Cleaning pigs, pp. 2 – 5, 2009. www.worldpipelines.com.

[8] 'Fluid-particle correlated motion and turbulent energy transfer in a two-dimensional particle-laden flow', S. Horender and Y. Hardalupas, *Chemical Engineering Science*, **65,** 5075-5091, 2010.

[9] 'Interface interaction in a turbulent vertical channel flow laden with heavy particles-Part I: Numerical methods and particle dispersion properties', B. Wang, *International Journal of Heat and Mass Transfer*, **53,** 2506-2521, 2010.

[10] 'Eulerian-Lagrangian modeling of turbulent liquid-solid slurries in horizontal pipes', J. Capecelatro and O. Desjardins, *International Journal of Multiphase Flows*, **55,** 64-79, 2013.

[11] 'Solid velocity and concentration fluctuations in highly concentrated liquid-solid (slurry) pipe flows', S.A. Hahsemi, A. Sadighian, S.I.A. Shah and R.A. Sanders, *International Journal of Multiphase Flows* **66,** 46-61, 2014.

[12] 'Numerical prediction of fully-suspended slurry flows in horizontal pipes', G.V. Messa, M. Malin, and S. Malavasi, *Powder Technology*, **256,** 61-70, 2014.

[13] 'A comprehensive review of solid particle erosion modelling for oil and gas wells and pipeline applications', M. Parsi, K. Najmi, F. Najafifard, S. Hassani, B.S. McLaury and S.A. Shirazi, *Journal of Natural Gas and Engineering Science*, **21,** 850-873, 2014.

[14] 'Sand suspension deposition in horizontal low concentration pipe flows', J.A.R. Boulanger and C.Y. Wong, *Granular Matter*, **18,** 15-24, 2016. DOI 10.1007/s10035-016-0616-2.

[15] 'Simulation and analysis of multiphase transport and reaction in segmented flows microreactors', L. Yang, M.J. Nieves-Remacha and K.F. Jensen, *Chemical Engineering Science*, **169,** 106-116, 2016.

[16] 'Modelling particle transport in gas-oil-sand multiphase flows and its applications to production operations', O.O. Bello, Ph.D. Thesis, 2008, Clausthal University of Technology, Clausthal.

[17] 'A comparative study on sand transport modeling for horizontal multiphase pipeline', K.W. Choong, L.P. Wen, L.L. Tiong, F. Anosike, M.A. Shoushtari and I.M. Saaid, (2014).. *Research Journal of Applied Sciences, Engineering and Technology* **7,** 6, 1017-1024.

[18] 'Vibration sensor approaches for sand detection in oil-water-sand multiphase flows', K. Wang, Z. Liu, G. Liu, L. Yi, P. Liu, M. Chen and S. Peng, *Powder Technology*, **276,** 183 – 192, 2015.

[19] 'The engineering science of oil pipelines Science Media Centre of Canada', Mimeograph, pp. 1 – 5, 2011.

[20] 'Investigation of corrosion in the pipeline using toeflt in an Iran refinery', A. Samini and S. Zarinabadi, *International Journal of Innovation and Applied Studies*, **1,** 2, 153-159, 2012.

[21] 'Corrosion and cathodic protection theory', B. James and P. Bushman, *International Journal of Renewable Energy Research*, **4:** 3-10, 2014.

[22] 'Review of Sand Production Prediction Models', H. Rahmati, M. Jafarpour, S. Azadbakht, A. Nouri, H. Vaziri, D. Chan and Y. Xia, *Journal of Petroleum Engineering*, pp. 1-16, 2013. http://dx.doi.org/10.1155/2013/864981.

[23] 'Modeling of sand and crude oil flow in horizontal pipes during crude oil transportation', S.E. Sanni, A.S. Olawale and S.S. Adefila, *Journal of Engineering*, **2015,** 1-7, 2017.

[24] ‘Mechanisms for Controlling Sand-Induced Corrosion in Horizontal Pipe Flow of Sand, Crude Oil and Water’, S.E. Sanni, S.S. Adefila, A.N. Anozie and O. Agboola, *The Open Petroleum Engineering Journa*l, Article in Press, 2017.

[25] ‘Fractured reservoir history matching improved based on artificial intelligent’, H.R. Sayyed, Z. Ghasem, B. Mehdi, M. Bahman and S.D. Ebrahim, *Petroleum*, article in press, 2016. DOI: 10.1016/j.petlm.2016.09.001.